

WEC-Sim

THEORY MANUAL

Version 1.1

April 3, 2015

License

Copyright 2014 the National Renewable Energy Laboratory and Sandia Corporation

Licensed under the Apache License, Version 2.0 (the "License"); you may not use this file except in compliance with the License. You may obtain a copy of the License at:

<http://www.apache.org/licenses/LICENSE-2.0>

Unless required by applicable law or agreed to in writing, software distributed under the License is distributed on an "AS IS" BASIS, WITHOUT WARRANTIES OR CONDITIONS OF ANY KIND, either express or implied. See the License for the specific language governing permissions and limitations under the License.

Acknowledgments

WEC-Sim is a multilaboratory project sponsored by the U.S. Department of Energy's Wind and Water Power Technologies Office. WEC-Sim code development is a collaboration between the National Renewable Energy Laboratory (NREL)¹ and Sandia National Laboratories (SNL)².

Principal Developers

Kelley Ruehl (SNL)
Carlos Michelen (SNL)

Michael Lawson (NREL)
Yi-Hsiang Yu (NREL)

Contributors

Nathan Tom (NREL)
Sam Kanner (University of
California at Berkeley)

Adam Nelessen (Georgia Tech)
Chris McComb (Carnegie
Mellon University)



¹The National Renewable Energy Laboratory is a national laboratory of the U.S. Department of Energy, Office of Energy Efficiency and Renewable Energy, operated by the Alliance for Sustainable Energy, LLC, under contract No. DE-AC36-08GO28308.

²Sandia National Laboratories is a multi-program laboratory managed and operated by Sandia Corporation, a wholly owned subsidiary of Lockheed Martin Corporation, for the U.S. Department of Energy's National Nuclear Security Administration under contract DE-AC04-94AL85000.

Contents

1	Introduction To WEC-Sim	4
2	Theory	5
2.1	Introduction	5
2.2	Boundary Element Method	5
2.3	Coordinate System in WEC-Sim	6
2.4	Time-Domain Numerical Method	6
2.4.1	Sinusoidal Steady-State Response Scenario	7
2.4.2	Convolution Integral Formulation	7
2.4.3	Wave Spectrum	8
2.4.4	Ramp Function	11
2.5	Power Take-off Forces	11
2.6	Mooring Forces	12
2.7	Viscous Drag	12

Chapter 1: Introduction To WEC-Sim

WEC-Sim (Wave Energy Converter SIMulator) is an open source wave energy converter (WEC) simulation tool. The code is developed in MATLAB and Simulink using the multi-body dynamics solver SimMechanics. WEC-Sim has the ability to model devices that are comprised of rigid bodies, power-take-off (PTO) systems, and mooring systems. Hydrodynamic forces are modeled using a radiation and diffraction method, and the system dynamics is performed in the time domain by solving the governing WEC equations of motion in 6 degrees of freedom (DOF). In this manual, the theory of WEC-Sim is described.

Chapter 2: Theory

2.1 Introduction

Modeling a WEC involves the interaction between the incident waves, device motion, PTO mechanism, and mooring (Figure 2.1). WEC-Sim uses a radiation and diffraction method [1, 2] to predict power performance and design optimization. The radiation and diffraction method generally obtains the hydrodynamic forces from a frequency-domain boundary element method (BEM) solver using linear coefficients to solve the system dynamics in the time domain.

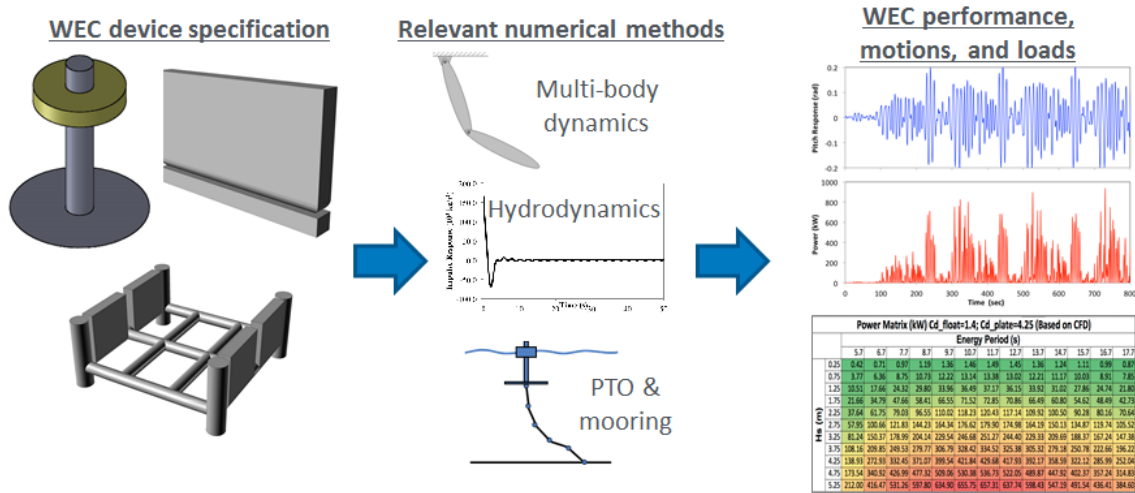


Figure 2.1: Methodology for WEC-Sim

2.2 Boundary Element Method

A common approach to determining the hydrodynamic forces is to presume that they are the sum of incident, radiated, and diffracted wave components. These forcing components are modeled using linear coefficients ideally obtained from a frequency-domain potential flow BEM solver (e.g., WAMIT [3], AWQA-FER [4], and Nemoh [5]). The BEM solutions are obtained by solving the Laplace equation for the velocity potential, which assumes the flow is inviscid, incompressible, and irrotational. More details on the theory for the frequency-domain BEM can be found in [3].

2.3 Coordinate System in WEC-Sim

Figure 2.2 illustrates a 3-D floating point absorber subject to incoming waves in water. The figure also defines the coordinates and the 6 DOF in WEC-Sim. The WEC-Sim coordinate system assumes that the X axis is in the direction of wave propagation if the wave heading angle is equal to zero. The Z axis is in the vertical upwards direction, and the Y axis direction is defined by the right-hand rule. In the vectors and matrices used in the code, surge (x), sway (y), and heave (z) correspond to the first, second and third position respectively. Roll (Rx), Pitch (Ry), and Yaw (Rz) correspond to the fourth, fifth, and sixth position respectively.

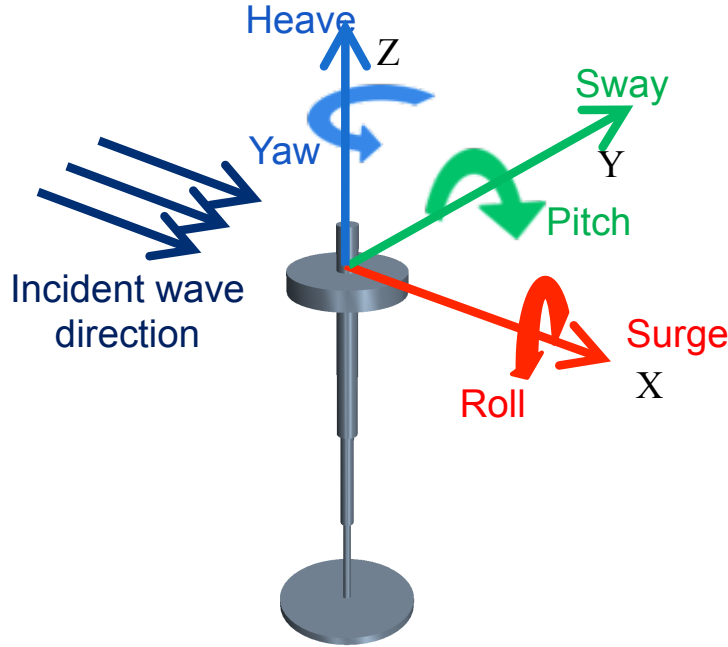


Figure 2.2: Sketch defining the coordinate system

2.4 Time-Domain Numerical Method

The dynamic response of the system was calculated by solving the equation of motion for WEC systems [2, 6]. The equation of motion for a floating body, about its center of gravity, can be given as:

$$m\ddot{\mathbf{X}} = \mathbf{F}_{ext} + \mathbf{F}_{rad} + \mathbf{F}_{PTO} + \mathbf{F}_v + \mathbf{F}_B + \mathbf{F}_m, \quad (2.1)$$

where $\ddot{\mathbf{X}}$ is the (translational and rotational) acceleration vector of the device, m is the mass matrix, \mathbf{F}_{ext} is the wave excitation force vector, \mathbf{F}_{rad} is the force vector resulting from wave radiation, \mathbf{F}_{PTO} is the PTO force vector, \mathbf{F}_v is the viscous damping force vector, \mathbf{F}_B is the

net buoyancy restoring force vector, and F_m is the force vector resulting from the mooring connection.

Both F_{ext} and F_{rad} are calculated from values provided by the frequency-domain BEM solver. The radiation term includes an added-mass and wave damping term associated with the acceleration and velocity of the floating body, respectively. The wave excitation term includes a Froude–Krylov force component generated by the undisturbed incident waves and a diffraction component that results from the presence of the floating body. WEC-Sim can be used for regular and irregular wave simulations, but note that F_{ext} and F_{rad} are calculated differently for sinusoidal steady-state response scenarios and random sea simulations. The sinusoidal steady-state response is often used for simple WEC designs with regular incoming waves. However, for random sea simulations or any simulations where fluid memory effects of the system are essential, the convolution integral method is recommended to represent the fluid memory retardation force on the floating body.

2.4.1 Sinusoidal Steady-State Response Scenario

This approach assumes that the system response is in sinusoidal steady-state form, and is only valid for regular wave simulations. The radiation term can be calculated using the added mass and the wave radiation damping term for a given wave frequency, which is obtained from

$$F_{rad} = -A(\omega_r)\ddot{X} - B(\omega_r)\dot{X}, \quad (2.2)$$

where $A(\omega_r)$ and $B(\omega_r)$ are the added-mass and wave radiation damping matrices, respectively. ω_r is the wave frequency (in rad/sec), and \dot{X} is the velocity vector of the floating body.

The free surface profile is based on linear wave theory for a given wave height, wave frequency, and water depth. The regular wave excitation force is obtained from

$$F_{ext} = \Re \left[R_f \frac{H}{2} F_X(\omega_r) e^{i(\omega_r t)} \right], \quad (2.3)$$

where \Re denotes the real part of the formula, R_f is the ramp function, H is the wave height, and F_X is the excitation vector, including the magnitude and phase of the force.

2.4.2 Convolution Integral Formulation

To include the fluid memory effect on the system, the convolution integral calculation, which is based upon the Cummins equation [7], is used. The radiation term can be calculated by

$$F_{rad} = -A_\infty \ddot{X} - \int_0^t K(t - \tau) \dot{X}(\tau) d\tau, \quad (2.4)$$

where A_∞ is the added mass matrix at infinite frequency and K is the impulse response function.

For regular waves, Eq. 2.3 is used to calculate the wave excitation force. For irregular waves, the free surface elevation is constructed from a linear superposition of a number of regular wave components. It is often characterized using a wave spectrum (Figure 2.3) that describes the wave energy distribution over a range of wave frequencies, characterized by a significant wave height and peak wave period. The irregular excitation force can be calculated as the real part of an integral term across all wave frequencies as follows

$$F_{ext} = \Re \left[R_f F_X(\omega_r) e^{i(\omega_r t + \phi)} \int_0^\infty \sqrt{2S(\omega_r)} d\omega_r \right], \quad (2.5)$$

where S is the wave spectrum and ϕ is a random phase angle.

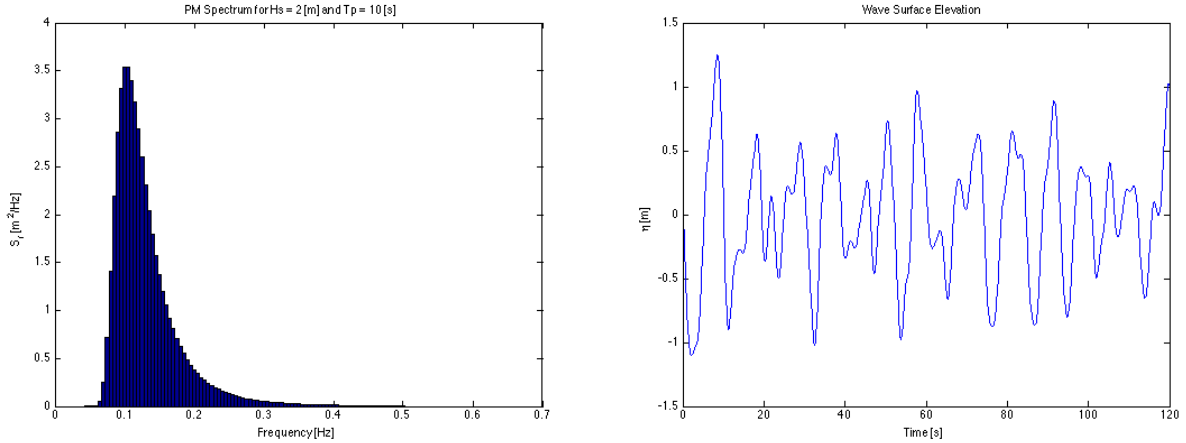


Figure 2.3: An example of wave spectrum and irregular wave elevation generated by WEC-Sim (Pierson–Moskowitz spectrum)

2.4.3 Wave Spectrum

The ability to generate regular waves provides an opportunity to observe the response of a model under specific conditions. Sea states with constant wave heights and periods are rarely found outside wave tank test. Normal sea conditions are more accurately represented by random-wave time series that model the superposition of various wave forms with different amplitudes and periods. This superposition of waves is characterized by a sea spectrum. Through statistical analysis, spectra are characterized by specific parameters such as significant wave height, peak period, wind speed, fetch length, and others. The common types of spectra that are used by the offshore industry are discussed in the following sections. The

general form of the sea spectrums available in WEC-Sim is given by:

$$S(f) = Af^{-5} \exp[-Bf^{-4}] \quad , \quad (2.6)$$

where f is the wave frequency (in Hertz) and \exp stands for the exponential function.

Pierson–Moskowitz

One of the simplest spectra was proposed by [8]. It assumed that after the wind blew steadily for a long time over a large area, the waves would come into equilibrium with the wind. This is the concept of a fully developed sea, where a "long time" is roughly 10,000 wave periods, and a "large area" is roughly 5,000 wave-lengths on a side. The spectrum is calculated from

$$S(f) = \frac{\alpha_{PM}g^2}{(2\pi)^4} f^{-5} \exp\left[-\frac{5}{4}\left(\frac{f_p}{f}\right)^4\right] \quad , \quad (2.7)$$

$$A = \frac{\alpha_{PM}g^2}{(2\pi)^4} \quad , \quad B = \frac{5}{4}f_p^4 \quad , \quad (2.8)$$

where $\alpha_{PM} = 0.0081$, g is gravitational acceleration, and f_p is the peak frequency of the spectrum. However, this spectrum representation does not allow the user to define the significant wave height. To facilitate the creation of a power matrix, in WEC-Sim the α_{PM} coefficient was calculated such that the desired significant wave height of the sea state was met. The α_{PM} fit was calculated as follows:

$$\alpha_{PM} = \frac{H_{m0}^2}{16 \int_0^\infty S^*(f) df} \quad , \quad (2.9)$$

$$S^*(f) = \frac{g^2}{(2\pi)^4} f^{-5} \exp\left[-\frac{5}{4}\left(\frac{f_p}{f}\right)^4\right] \quad . \quad (2.10)$$

Note that related to the spectrum is a series of characteristic numbers called the spectral moments. These numbers, denoted m_k , $k = 0, 1, 2, \dots$ are defined as

$$m_k = \int_0^\infty f^k S(f) df \quad . \quad (2.11)$$

The spectral moment, m_0 is the variance of the free surface, which allows one to define

$$H_{m0} = 4\sqrt{m_0} \quad . \quad (2.12)$$

Bretschneider Spectrum

This two-parameter spectrum is based on significant wave height and peak wave frequency. For a given significant wave height, the peak frequency can be varied to cover a range of conditions including developing and decaying seas. In general, the parameters depend on

wind speed (most important), wind direction, as well as fetch and locations of storm fronts. The spectrum is given as

$$S(f) = \frac{H_{m0}^2}{4} (1.057 f_p)^4 f^{-5} \exp \left[-\frac{5}{4} \left(\frac{f_p}{f} \right)^4 \right] , \quad (2.13)$$

$$A = \frac{H_{m0}^2}{4} (1.057 f_p)^4 \approx \frac{5}{16} H_{m0}^2 f_p^4 , \quad (2.14)$$

$$B = (1.057 f_p)^4 \approx \frac{5}{4} f_p^4 , \quad (2.15)$$

where H_{m0} is the significant wave height which is generally defined as the mean wave height of the one third highest waves.

JONSWAP (Joint North Sea Wave Project) Spectrum

Spectrum used in WEC-Sim

The spectrum was purposed by Hasselmann et al. [9], and the original formulation was given as

$$S(f) = \frac{\alpha_j g^2}{(2\pi)^4} f^{-5} \exp \left[-\frac{5}{4} \left(\frac{f_p}{f} \right)^4 \right] \gamma^\Gamma$$

$$\Gamma = \exp \left[-\left(\frac{\frac{f}{f_p} - 1}{\sqrt{2}\sigma} \right)^2 \right] , \sigma = \begin{cases} 0.07 & f \leq f_p \\ 0.09 & f > f_p \end{cases} , \quad (2.16)$$

$$A = \frac{\alpha_j g^2}{(2\pi)^4} , \quad B = \frac{5}{4} f_p^4 , \quad (2.17)$$

where α_j is a nondimensional variable that is a function of the wind speed and fetch length.

Empirical fits were applied in an attempt to find a mean value that would capture the spectral shape of most measured sea states. To fit α_j to match the desired significant wave height the following calculation must be performed

$$\alpha_j = \frac{H_{m0}^2}{16 \int_0^\infty S^*(f) df} , \quad (2.18)$$

$$S^*(f) = \frac{g^2}{(2\pi)^4} f^{-5} \exp \left[-\frac{5}{4} \left(\frac{f_p}{f} \right)^4 \right] \gamma^\Gamma . \quad (2.19)$$

Spectrum purposed at ITTC

Another form of JONSWAP spectrum was purposed at the 17th International Towing Tank Conference (ITTC). It was defined as

$$S(f) = \frac{155}{(2\pi)^4} \frac{H_{m0}^2}{(0.834 T_p)^4} f^{-5} \exp \left[-\frac{5}{4} \left(\frac{f_p}{f} \right)^4 \right] \gamma^\Gamma$$

$$\approx \frac{310}{(2\pi)^4} H_{m0}^2 f_p^4 f^{-5} \exp \left[-\frac{5}{4} \left(\frac{f_p}{f} \right)^4 \right] \gamma^\Gamma , \quad (2.20)$$

$$\Gamma = \exp \left[-\left(\frac{\frac{f}{f_p} - 1}{\sqrt{2}\sigma} \right)^2 \right] , \quad \sigma = \begin{cases} 0.07 & f \leq f_p \\ 0.09 & f > f_p \end{cases} , \quad (2.21)$$

$$A = \frac{310}{(2\pi)^4} H_{m0}^2 f_p^4 , \quad B = \frac{5}{4} f_p^4 . \quad (2.22)$$

Figure 2.4 shows the comparison of the JONSWAP spectrum obtained from the α_j fit and the ITTC description. It is clear that the two methods have very good agreement.

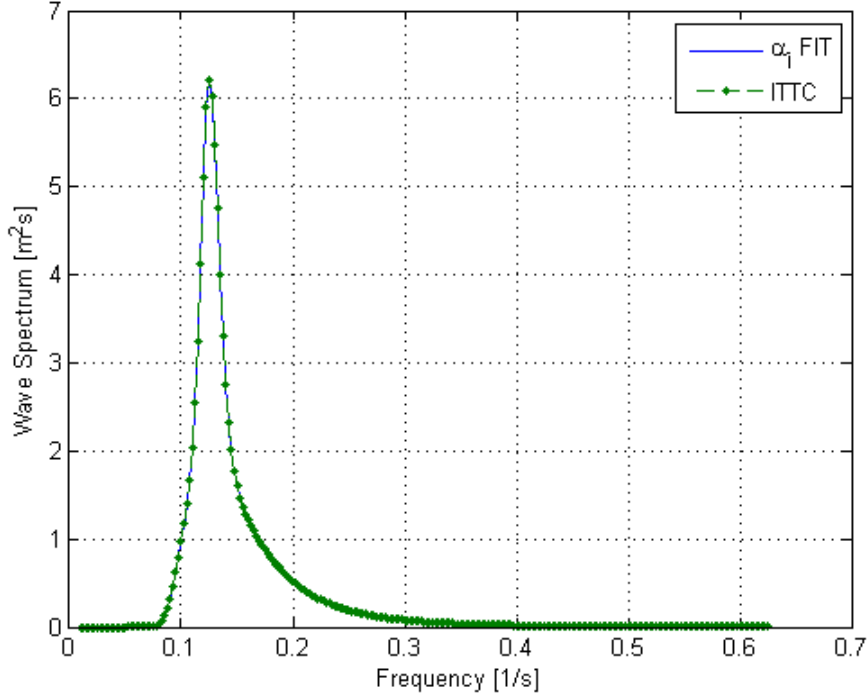


Figure 2.4: Comparison of α_j fit to the ITTC description of the JONSWAP spectrum with $H_{m0} = 2$ m and peak period (T_p) of 8 sec.

2.4.4 Ramp Function

A ramp function (R_f), necessary to avoid strong transient flows at the earlier time steps of the simulation, is used to calculate the wave excitation force. The ramp function is given by

$$R_f = \begin{cases} \frac{1}{2}(1 + \cos(\pi + \frac{\pi t}{t_r})), & \frac{t}{t_r} < 1 \\ 1, & \frac{t}{t_r} \geq 1 \end{cases}, \quad (2.23)$$

where t is the simulation time and t_r is the ramp time.

2.5 Power Take-off Forces

The PTO mechanism is represented as a linear spring-damper system, where the reaction force is given by:

$$F_{PTO} = -K_{PTO}X_{rel} - C_{PTO}\dot{X}_{rel}, \quad (2.24)$$

where K_{PTO} is the stiffness of the PTO, C_{PTO} is the damping of the PTO, and X_{rel} and \dot{X}_{rel} are the relative motion and velocity between two bodies. The power consumed by the PTO is given by:

$$P_{PTO} = -F_{PTO}\dot{X}_{rel} = \left(K_{PTO}X_{rel}\dot{X}_{rel} + C_{PTO}\dot{X}_{rel}^2 \right). \quad (2.25)$$

However, the relative motion and velocity between two bodies is out of phase by $\pi/2$, resulting in a time-averaged product of 0. This allows the absorbed power to be written as

$$P_{PTO} = C_{PTO}\dot{X}_{rel}^2. \quad (2.26)$$

2.6 Mooring Forces

The mooring load is represented using a linear quasi-static mooring stiffness, which can be calculated by

$$F_m = -K_m X, \quad (2.27)$$

where K_m is the stiffness matrix for the mooring system, and X is the response of the body.

2.7 Viscous Drag

Generally, the effect of viscosity on the WEC dynamics needs to be considered as neglecting this effect may lead to an overestimation of the power generation of the system, particularly when a linear model is applied. A common way of modeling the viscous damping is to add a (Morison-equation-type) quadratic damping term to the equation of motion;

$$F_V = \frac{1}{2}C_d\rho A_D\dot{X}|\dot{X}|, \quad (2.28)$$

where C_d is the viscous drag coefficient, ρ is the fluid density, and A_D is the characteristic area. The viscous drag coefficient for the device must be carefully selected [1, 2]; however, it is dependent on device geometry, scale, and relative velocity between the body and the flow around it. The drag coefficient becomes much larger when the Reynolds and the Keulegan–Carpenter number are smaller. Note that empirical data on the drag coefficient can be found in various literature and standards. The available data may, however, be limited to existing simple geometries. For practical point absorber geometry, the hydrodynamic forces may have to be evaluated by conducting wave tank tests or prescribed motion computational fluid dynamic simulations.

Bibliography

- [1] Y. Li and Y.-H. Yu, “A Synthesis of Numerical Methods for Modeling Wave Energy Converter-Point Absorbers,” *Renewable and Sustainable Energy Reviews*, vol. 16, no. 6, pp. 4352–4364, 2012.
- [2] A. Babarit, J. Hals, M. Muliawan, A. Kurniawan, T. Moan, and J. Krokstad, “Numerical Benchmarking Study of a Selection of Wave Energy Converters,” *Renewable Energy*, vol. 41, pp. 44–63, 2012.
- [3] C. Lee and J. Newman, “WAMIT User Manual,” Chestnut Hill, MA, USA, 2006.
- [4] “ANSYS Aqwa.” [Online]. Available: <http://www.ansys.com/Products/Other+Products/ANSYS+AQWA>
- [5] “Nemoh a Open source BEM.” [Online]. Available: <http://openore.org/tag/nemoh/>
- [6] J. D. Nolte and R. C. Ertekin, “Wave power calculations for a wave energy conversion device connected to a drogue,” *Journal of Renewable and Sustainable Energy*, vol. 6, no. 1, 2014.
- [7] W. Cummins, “The Impulse Response Function and Ship Motions,” David Taylor Model Basin-DTNSRDC, Tech. Rep., 1962.
- [8] W. J. Pierson and L. A. Moskowitz, “Proposed Spectral Form for Fully Developed Wind Seas Based on the Similarity Theory of S. A. Kitaigorodskii,” *Geophysical Research*, vol. 69, pp. 5181–5190, 1964.
- [9] K. Hasselman, T.P. Barnett, E. Bouws, H. Carlson, D.E. Cartwright, K. Enke, J.A. Ewing, H. Gienapp, D.E. Hasselmann, P. Kruseman, A. Meerburg, P. Mller, D.J. Olbers, K. Richter, W. Sell, and H. Walden, “Measurements of wind-wave growth and swell decay during the Joint North Sea Wave Project (JONSWAP),” German Hydrographic Institute, Tech. Rep. 12, 1973.